

Assessment of Sulfate and Chloride in Coastal Soil of Karachi and Their Impacts on Concrete Structure

Bisma Naz and Adnan Khan

Department of Geology, University of Karachi, Karachi 74900, Sindh, Pakistan

ABSTRACT

Background and Objective: Coastal corrosion due to sulphate and chloride invasion in concrete structures is common that reduces the life of concrete structures. Hence, selecting the type of cement is one effective measure. Therefore, the main objective of the present study is to determine the sulfate and chloride effects on concrete structures and to suggest cement types for the constructions accordingly.

Materials and Methods: For this purpose, soil samples ($n = 50$) were collected by using a hand auger at a depth of about $4 \text{ feet} \pm 0.5$. The physicochemical and textural characteristics of soil were assessed. Soil pH, Total Dissolved Salts (TDS) and water-soluble salts content (SO_4 and Cl^-) were determined. **Results:** Data reveal that the soil pH is circum-neutral to alkaline. TDS (range: 0.004-0.4%), chloride (range: 0.001-0.44%) and sulfate (range: 0.04-1.09%) concentrations also cover a wide variations. Sulfate concentration is influenced by the arid climate, soil texture and the occurrence of gypsum fragments. Results of statistical analysis show that soil salinity is mainly influenced by NaCl salts and by soil texture as well. **Conclusion:** It is concluded that Cl^- and SO_4 distribution is variable in the study area. Type II, V or I cement+7% silica fume or 20% fly ash is recommended in moderate to severe sulfate exposure sites, respectively. Whereas, Ordinary Portland Cement (OPC) is suggested for minimal sulfate exposure sites such as Benazir Abad Town.

KEYWORDS

Concrete deterioration, reinforcement corrosion, deleterious species, sulfate and chloride, Karachi coast, civil structures, type V cement, type II cement

Copyright © 2022 Bisma Naz and Adnan Khan. This is an open-access article distributed under the Creative Commons Attribution License, which permits unrestricted use, distribution and reproduction in any medium, provided the original work is properly cited.

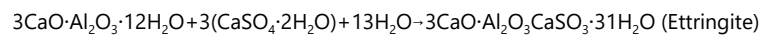
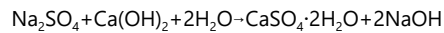
INTRODUCTION

Civil structures require a suitable foundation soil for long-term stability because the footings of structures are founded at depths underground¹. Most of the coastal areas in the world have problematic soil in terms of salinity, alkalinity, acid sulphate, water logging and sandy texture². Soil salinity is a major problem in arid and semi-arid regions of the world³⁻⁵ which is extremely inappropriate for construction⁶. The soil near to coast is often contaminated with sulphate and chloride due to seawater intrusion and invasion, which causes the decay of concrete structures particularly marine structures because of the migration of highly deleterious species (sulfate and chloride ions) into the concrete.



Soil stabilization is important for foundation development because most of the geotechnical problems are caused by weak soils with low strength and high compressibility⁷. Areas containing problematic soil such as clayey soil is stabilized by adding a cementing agent such as lime or cement⁸ to enhance their load-bearing capacity^{9,10}. However, in the presence of soluble sulphates in soil, the lime stabilization technique can contribute significantly to pavement failure and structural deterioration as well¹¹⁻¹³. Sulphate is a soil anion that forms from the dissolution of certain minerals like sodium sulphate (Na₂SO₄), gypsum (CaSO₄·2H₂O), magnesium sulphate (MgSO₄), anhydrite (CaSO₄) and barite (BaSO₄). Besides, gypsum remains the major form of sulphate found in soil which has a high capacity for swelling and a low strength when wet⁷. This soil causes serious structural damage.

When sulphate-rich soil is treated with lime or cement the cation exchange reaction takes place^{14,15}. In this process, clay releases ammonia at pH values > 10.5 and this ammonia interacts with Ca²⁺ (contained in lime or cement), soil sulphate ions and available soil water to form Calcium-Aluminate-Sulphate-Hydrate (CASH) i.e., Ettringite¹⁶⁻¹⁹ which damages the soil structure through mineral expansion during its precipitation²⁰. The chemical reaction related to sulfate attack are as follows:



On the other hand, corrosion of reinforcing steel in concrete is predominantly caused by chloride ions which may be contributed internally (concrete mixture ingredient) or externally from the environment. From the external environment, chloride ion diffuses through the concrete to the steel surface, leading to the deprivation of the protective Fe₂O₃ layer and ultimately causing reinforcement corrosion. It is well established that proper designing and construction of the foundation for mega infrastructures can prevent structural failure and post-construction issues²¹⁻²³. Hence, there is a dire need to investigate the quality of soil near to coast where the structure will be placed for over 100 years. Despite aggressive construction activities in coastal parts of Karachi City, no studies have been carried out so far on coastal soil salinity particularly sulfate and chloride hazards for construction. Therefore, the present study is aimed at assessing SO₄ and Cl⁻ the potential of soil in coastal areas of Karachi where housing schemes are rapidly growing. Coastal soil salinity patterns will be endorsed by the data of Pakistani coastal areas to support the global pattern of salinity variation.

MATERIALS AND METHODS

Study area: The study was carried out in January to December, 2020. The study area is located in the west of Karachi City near Mubarak Village and Sona Pass area between 24°51'17.3267"E to 24°55'48.4185"N and 66°41'5.4442"E to 66°52'23.9345"N. It lies on the east and southwest of the eastern flank of Cape Monze anticline and West of Lal Bakhar ridge (Fig. 1). The study site is mainly a plain area with a sparse vegetal cover of herbaceous plants. Sites in proximity to the coast are mainly affected by salt due to low-lying topography. The southwestern part near Hub River is mainly affected by seawater invasion where the river is replenished by salty seawater. The exposed rocks in the study area are mainly silici-clastic with subordinate limestone units of Nari and Gaj formations of the Oligocene and Miocene ages, respectively.

Soil sampling: Soil sampling was carried out by ASTM D-1452 standard procedure. Fifty soil samples were randomly collected along roadsides by using a hand auger (height: 5 feet) up to a depth of 4 feet because soil cover is thin due to rock exposure near-surface and low gradient. The sampling area was cleaned by shovel to remove surface debris and then an Auger boring was carried out by rotating the "T" handle of an auger in a vertical position from an unconsolidated deposit ranging from clayey sand to gravel. The

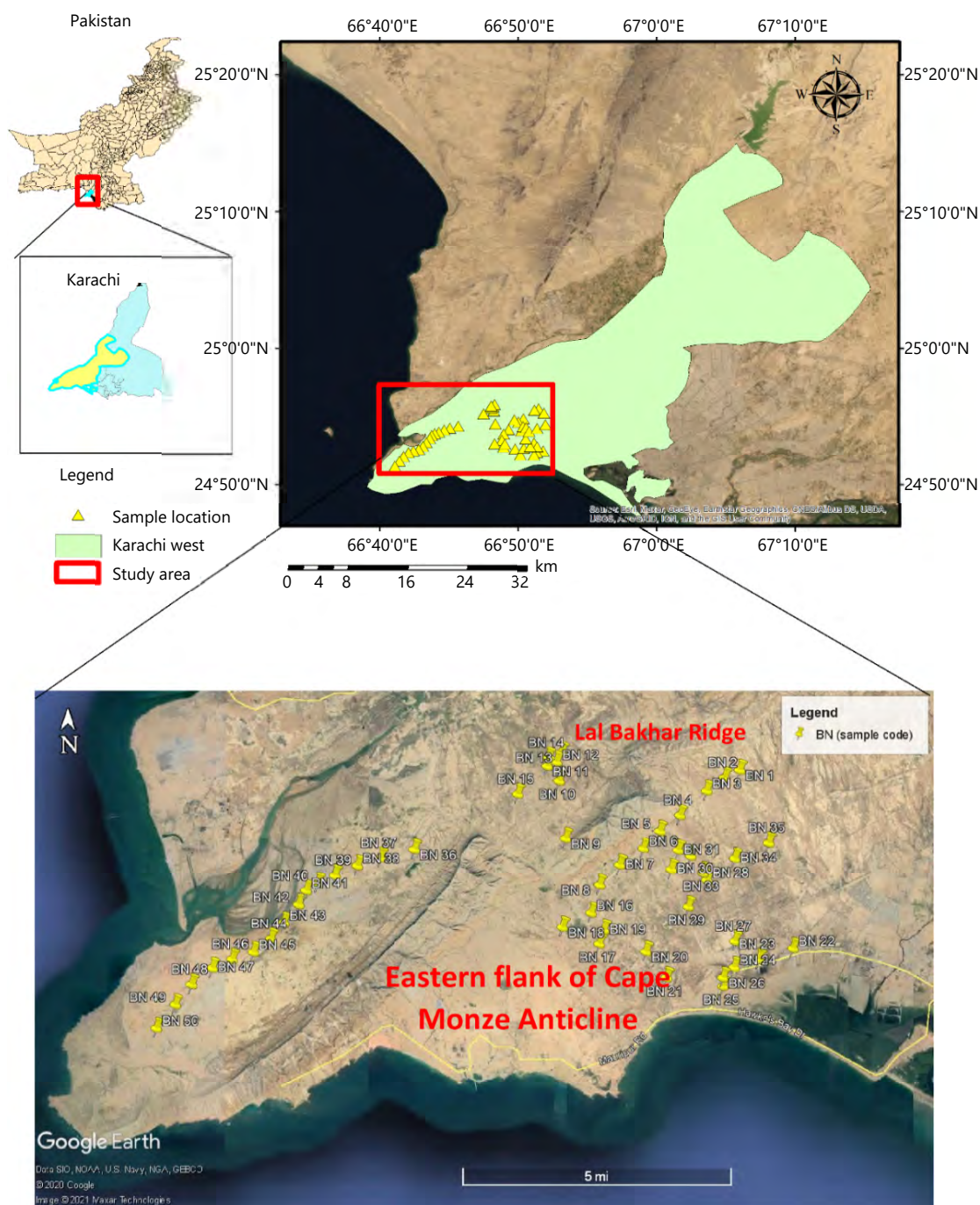


Fig. 1: Location map of study area and collected soil (n = 50) samples

auger was taken out from the hole and the excavated soil was collected in polyethene sample bags. The same procedure was repeated until the desired depth is reached. Approximately 1 kg of each disturbed soil sample was collected for laboratory investigation. The field coordinates of all sampling sites were noted by using the Global Positioning System (GPS) and plotted on Google Earth Map (Fig. 1).

Soil chemical analysis: Soil samples were carefully prepared for salinity measurements according to the Tex-620-J standard method. Samples were air-dried and screened through US standard #30 (0.59 mm) sieve. A solution of the sample in deionized water was prepared (1:10) and filtered by using #42 size filter paper to determine pH, total dissolved salts content, water-soluble sulfate and chloride concentrations

by standard gravimetric (ASTM C-1580) and titration method (ASTM D-512), respectively. The pH was measured in a 1:1 soil/H₂O extract using a pH meter (AD 111) following the standard (ASTM D-4972) procedure. The soil texture was analyzed by the dry sieving technique.

Statistical analysis: Statistical analysis of soil physicochemical parameters was carried out using SPSS 20 (Statistical Package for Social Science, IBM, Armonk, NY, USA). The study area map was drawn by using ARC Map 10.5 software.

RESULTS AND DISCUSSION

Physicochemical characteristics of collected soil: Results of physicochemical characteristics of collected soil samples have been summarized in Table 1. Data reveal that the soil pH varied from circumneutral to alkaline (range = 6.5-8.7, mean = 7.74 ± 0.8) whereas, a large number of samples (n = 40) are alkaline (range = 7.5-8.7). However, one sample (BN-17) has shown an extremely acidic pH (3.25) which is due to the deleterious occurrence of pyrite in this sample. Soil pH is generally associated with the pH of parent material and climate as well²⁴. The soil of the arid region has alkaline pH and the soil derived from calcareous material also shows a neutral to alkaline pH²⁵. Hence, alkalinity in the soil of the study area is due to the occurrence of limestone fragments from surrounding rocks and the presence of an arid climate. It is because in a dry environment leaching and weathering are less intense due to low rainfall.

High salinity in soil tends to cause corrosion of steel and concrete²⁶. TDS content is highly fluctuating in collected soil samples (n = 50) which span between 0.004-0.4% mean = 0.04 ± 0.069 (Table 2). Similarly, chloride distribution is also highly variable (range = 0.001-0.44%, mean = 0.05%). It is extremely high in samples collected from proximity to the sea where it is ranging between 0.1-0.44%. Hence, the highly variable chloride concentration in the soil of the study area is due to the change in soil mineral composition and the presence of NaCl salts. Excessive concentration of chloride ions in the soil of the study area is prone to corrode the reinforcing steel in concrete and subsequently reduce the strength and serviceability of the structure^{27,28}. Sulfate concentration is also fluctuating between extremely high to low sulfate regimes (range = 0.04-1.09%, mean = 0.25 ± 0.17). Soil sulfate concentration depends on the clay content, clay type and climate²⁹. Sulfate concentration increases with depth due to the presence of high clay content and Fe and Al oxides in the subsoil. It is observed that sulfate concentration in one-fifth of collected samples from the study area is reported to increase with increasing clay content because clay content strongly influences the soil and chemical interaction. After all, a small particle size has a large surface area which tends to have a high cation exchange capacity³⁰. Moreover, the exchange capacity of soil largely depends on the type of clay mineral as well³¹. Clay in the study area is mainly derived from the gypsiferous shale unit of Nari and Gaj formations which have been deposited in shallow marine environments³². Likewise, climate also influences the soil sulfate concentration²⁹. The soil of arid climatic regions usually has a large number of water-soluble salts such as Cl⁻ and SO₄²⁻ and CO₃³³. Since sulfate concentration in the soil of the study area is influenced by increasing clay content and arid climate.

Statistical analysis of coastal soil

Anion interrelationship: Statistical results of collected samples (n = 50) have been listed in Table 3. Data reveal a significant positive correlation of TDS with chloride (r = 0.65 at p < 0.01) suggesting that TDS is mainly influenced by NaCl which is controlled by various factors including water table rise from a saline aquifer in low-lying areas and seawater invasion^{34,35}.

Significant positive correlation of TDS (r = 0.361 at p = 0.01 level) and Cl (r = 0.538 at p = < 0.01) with clay content is due to the presence of electrically charged sites on clay surfaces which attract and hold the ions firmly³⁶. Moreover, the significant positive correlation of clay with depth (r = 0.327 at p < 0.05) is indicating that clay content is increasing with depth. In addition, clay also shows a positive correlation with TDS

Table 1: Physicochemical characteristics of collected soil samples (n=50)

Sample codes	Depth feet	pH	TDS (%)	Cl (%)	SO ₄ (%)	Clay (%)
BN 1	3	7.6	0.013	0.01	0.2	17
BN 2	3	8.7	0.009	0.0035	0.22	13.8
BN 3	2	8.13	0.015	0.011	0.21	13
BN 4	2	7.84	0.026	0.0035	0.31	8.6
BN 5	3	7.86	0.006	0.002	0.38	7.6
BN 6	3	7.93	0.005	0.002	0.2	4
BN 7	3	8.18	0.012	0.01	0.43	7.2
BN 8	3	8.21	0.024	0.02	0.35	10.6
BN 9	3	8.53	0.009	0.0035	0.34	7.5
BN 10	4	8.21	0.008	0.0035	0.08	6.6
BN 11	4	6.7	0.006	0.01	0.04	6.9
BN 12	4	7.89	0.01	0.012	0.04	0.8
BN 13	4	8.14	0.007	0.005	0.05	6.9
BN 14	4	8.03	0.006	0.0035	0.23	9.7
BN 15	4	6.32	0.008	0.0035	0.06	100
BN 16	4	8.25	0.03	0.025	0.16	100
BN 17	4	3.25	0.02	0.018	0.42	5.3
BN 18	4	8.0	0.005	0.0053	0.25	16
BN 19	4	8.0	0.01	0.0053	0.16	18
BN 20	4	8.33	0.006	0.02	0.24	41
BN 21	4	8.1	0.01	0.01	0.2	27
BN 22	3	7.84	0.09	0.11	0.37	100
BN 23	4	7.89	0.07	0.07	0.35	100
BN 24	3	7.8	0.09	0.08	0.4	9.8
BN 25	4	8.25	0.4	0.44	0.25	100
BN 26	4	8.35	0.04	0.01	0.21	100
BN 27	4	7.21	0.3	0.36	0.39	100
BN 28	4	7.65	0.23	0.2	0.54	99
BN 29	4	8.07	0.006	0.002	0.2	21
BN 30	4	8.03	0.005	0.001	0.13	19
BN31	4	8.32	0.025	0.02	0.1	19
BN 32	4	8.13	0.01	0.0035	0.2	22
BN 33	3	8.1	0.02	0.002	0.2	14.5
BN 34	4	8.1	0.004	0.002	0.31	8.9
BN 35	4	6.25	0.1	0.11	0.36	51
BN 36	4	7.39	0.01	0.01	0.28	23
BN 37	4	7.8	0.006	0.0035	0.4	9.3
BN 38	4	6.8	0.01	0.005	0.14	10.26
BN 39	4	8.3	0.1	0.1	0.24	35
BN 40	4	7.62	0.1	0.085	0.2	59.2
BN 41	4	7.51	0.12	0.15	0.33	17.6
BN 42	4	7.07	0.08	0.11	0.08	26
BN 43	4	7.63	0.18	0.2	0.41	36
BN 44	4	8.04	0.02	0.016	0.07	22
BN 45	4	7.6	0.13	0.13	0.32	33.45
BN 46	4	8.14	0.012	0.01	0.33	4
BN 47	4	8.04	0.016	0.01	0.07	13.8
BN 48	4	7.04	0.16	0.16	0.13	20
BN 49	4	7.74	0.13	0.04	1.09	29.1
BN 50	4	7.8	0.054	0.06	0.06	9.9

Sample code number is represented by the symbol (BN)

Table 2: Statistical descriptive of collected soil samples (n = 50)

Parameters	Statistics			
	Minimum	Maximum	Mean	Std. deviation
pH	3.25	8.70	7.73	0.8
TDS (%)	0.004	0.4	0.04	0.069
Cl (%)	0.001	0.44	0.05	0.09
SO ₄ (%)	0.04	1.09	0.25	0.17

Table 3: Correlation matrix of collected samples (n = 50)

Correlations		pH	TDS	SO ₄	Cl	Sand	Clay	Depth
Spearman's rho								
pH	Correlation coefficient	1						
	Sig. (2-tailed)							
	N	50						
TDS	Correlation coefficient	-0.128	1					
	Sig. (2-tailed)	0.375						
	N	50	50					
SO ₄	Correlation coefficient	-0.096	0.124	1				
	Sig. (2-tailed)	0.508	0.391					
	N	50	50	50				
Cl	Correlation coefficient	-0.292*	0.650**	0.27	1			
	Sig. (2-tailed)	0.039	0	0.058				
	N	50	50	50	50			
Sand	Correlation coefficient	0.233	-0.089	0.114	-0.149	1		
	Sig. (2-tailed)	0.104	0.538	0.43	0.301			
	N	50	50	50	50	50		
Clay	Correlation coefficient	-0.089	0.361**	0.119	0.538**	-0.164	1	
	Sig. (2-tailed)	0.537	0.01	0.411	0	0.256		
	N	50	50	50	50	50	50	
Depth	Correlation coefficient	-0.198	0.005	-0.262	0.255	-0.24	0.327*	1
	Sig. (2-tailed)	0.167	0.974	0.067	0.074	0.094	0.021	
	N	50	50	50	50	50	50	50

*Correlation is significant at the 0.05 level (2-tailed) and **0.01 level (2-tailed)

content ($r = 0.36$) showing that TDS is also increasing with depth. However, a weak correlation is due to the collection of samples from a constant depth (i.e., 4 feet). Since the footings of the structures are founded at a depth of about 4 feet where increasing clay content with depth can cause significant risk to infrastructure due to the high salt adsorption capacity of clay. Since the large number of samples collected from about 4 feet has a TDS content of $\pm 0.1\%$ which indicates that most of the sites are vulnerable to concrete work.

Statistical analysis of samples with elevated TDS (up to 0.4%): The high TDS samples ($n = 8$) have been statistically analyzed and listed in Table 4. Data revealed that pH has an insignificant positive correlation with TDS ($r = 0.559$ at $p > 0.05$), Na ($r = 0.342$ at $p > 0.05$ level) and Cl ($r = 0.306$ at $p > 0.05$ level) which is attributed to the fact that in calcareous soil pH increases with increasing salinity due to the presence of sodium ion. Na^+ react with carbonate and bicarbonate ions of the calcareous matrix in soil which is hydrolyzed at $\text{pH} > 8.8$ showing the direct relationship between soil salinity and pH ³⁷.

A positive correlation of sulfate with calcium ($r = 0.436$ at $p > 0.05$) indicates the presence of gypsum and the release of sulfate ion in soil solution at alkaline pH conditions is revealed by a positive correlation between sulfate and PH ($r = 0.429$ at $p > 0.05$). The significant strong relationship of TDS with Na ($r = 0.927$) and Cl ($r = 0.873$ at $p = 0.01$) suggests that NaCl salts are the source of extremely high TDS in soil samples. TDS is also highly associated with clay content ($r = 0.793$) suggesting that salinity in the soil is caused by relatively high clay content which is more prevalent at sea. Whereas, the negative correlation of sand with TDS ($r = -0.873$ at $p = 0.01$ level) clearly shows that increasing salinity is not controlled by the sand fraction in soil.

Statistical analysis of samples having low TDS content (<0.001%): Statistical correlation of low TDS samples has been listed in Table 5 which shows that clay content is positively correlated with Ca ($r = 0.64$ at $p > 0.05$) because calcium is the dominant cation in calcareous soil³⁸. A strong positive correlation of Na with pH ($r = 0.743$) and SO₄ ($r = 0.724$) supports the release of sodium from silicate minerals at alkaline pH where it pairs with SO₄ due to having a high amount of sulfate in these samples. The positive correlation of sand content with low TDS ($r = 0.402$ at $p > 0.05$) supports that salt does not accumulate in

Table 4: Statistical correlation analysis of high TDS samples (n = 8)

Correlations		pH	TDS	Ca	Na	SO ₄	Cl	Sand	Clay	Depth
Spearman's rho										
pH	Correlation coefficient	1.000								
	Sig. (2-tailed)									
	N	7								
TDS	Correlation coefficient	0.559	1.000							
	Sig. (2-tailed)	0.192								
	N	7	7							
Ca	Correlation coefficient	0.109	0.303	1.000						
	Sig. (2-tailed)	0.816	0.509							
	N	7	7	7						
Na	Correlation coefficient	0.342	0.927**	0.055	1.000					
	Sig. (2-tailed)	0.452	0.003	0.907						
	N	7	7	7	7					
SO ₄	Correlation coefficient	0.429	-0.144	0.436	-0.342	1.000				
	Sig. (2-tailed)	0.337	0.758	0.328	0.452					
	N	7	7	7	7	7				
Cl	Correlation coefficient	0.306	0.873*	0.110	0.964**	-0.306	1.000			
	Sig. (2-tailed)	0.504	0.010	0.814	0.000	0.504				
	N	7	7	7	7	7	7			
Clay	Correlation coefficient	0.714	0.793*	-0.055	0.721	0.000	0.577	1.000		
	Sig. (2-tailed)	0.071	0.033	0.908	0.068	1.000	0.175			
	N	7	7	7	7	7	7	7		
Sand	Correlation coefficient	-0.721	-0.873*	-0.138	-0.791*	-0.144	-0.682	-0.955**	1.000	
	Sig. (2-tailed)	0.068	0.010	0.769	0.034	0.758	0.092	0.001		
	N	7	7	7	7	7	7	7	7	
Depth	Correlation coefficient									
	Sig. (2-tailed)									
	N	7	7	7	7	7	7	7	7	7

**Correlation is significant at the 0.01 level (2-tailed) and *0.05 level (2-tailed)

Table 5: Statistical analysis of low TDS samples (n = 12)

Correlations		pH	TDS	SO ₄	Cl	Ca	Na	Sand	Clay
Spearman's rho									
pH	Correlation coefficient	1.000							
	Sig. (2-tailed)								
	N	11							
TDS	Correlation coefficient	0.176	1.000						
	Sig. (2-tailed)	0.606							
	N	11	11						
SO ₄	Correlation coefficient	0.200	-0.115	1.000					
	Sig. (2-tailed)	0.555	0.735						
	N	11	11	11					
Cl	Correlation coefficient	0.081	0.160	0.134	1.000				
	Sig. (2-tailed)	0.812	0.638	0.695					
	N	11	11	11	11				
Na	Correlation coefficient	0.743**	0.009	0.724*	0.247	1.000			
	Sig. (2-tailed)	0.009	0.978	0.012	0.465				
	N	11	11	11	11	11			
Ca	Correlation coefficient	0.248	-0.366	0.374	0.295	0.333	1.000		
	Sig. (2-tailed)	0.463	0.269	0.257	0.379	0.318			
	N	11	11	11	11	11	11		
Clay	Correlation coefficient	-0.145	-0.060	0.027	0.253	-0.118	0.640*	1.000	
	Sig. (2-tailed)	0.670	0.861	0.937	0.452	0.729	0.034		
	N	11	11	11	11	11	11	11	
Sand	Correlation coefficient	0.373	0.402	-0.055	0.086	0.178	-0.360	-0.573	1.000
	Sig. (2-tailed)	0.259	0.220	0.873	0.801	0.601	0.277	0.066	
	N	11	11	11	11	11	11	11	11

**Correlation is significant at the 0.01 level (2-tailed) and *0.05 level (2-tailed)

Table 6: Grain size distribution of samples (n = 50)

Sample codes	Colors	Gravel (%) MESH 8	Sand (%) MESH 170	Silt and clay (%) PAN	Total (%)
BN 1	Earthy brown	-	82	17	99
BN 2	Greenish brown	-	85.7	13.8	99.5
BN 3	Earthy brown	-	85	13	98
BN 4	Earthy brown	23.2	67.6	8.6	99.4
BN 5	Greenish grey	-	90.7	7.6	98.3
BN 6	Earthy brown	39	56	4	99
BN 7	Earthy brown	-	92	7.2	99.2
BN 8	Greenish brown	17.3	70.6	10.6	98.5
BN 9	Earthy brown	-	91.9	7.5	99.4
BN 10	Greenish brown	-	92	6.6	98.6
BN 11	Earthy brown	-	92.7	6.9	99.6
BN 12	Greenish brown	-	99	0.8	99.8
BN 13	Earthy brown	-	92.4	6.9	99.3
BN 14	Earthy brown	-	89.9	9.7	99.6
BN 15	Earthy brown	30.2	68.8	0.6	99.6
BN 16	Yellowish brown	-	-	100	100
BN 17	Earthy brown	32.8	61.4	5.3	99.5
BN 18	Earthy brown	11.44	72.2	16.13	99.8
BN 19	Earthy brown	-	81.85	17.7	99.5
BN 20	Earthy brown	-	58.3	41.0	99.3
BN 21	Greenish brown	-	72.8	26.8	99.6
BN 22	Greenish brown	-	-	100	100
BN 23	Greenish brown	-	-	100	100
BN 24	Greyish green	37.2	52.9	9.8	99.9
BN 25	Greenish brown	-	-	100	100
BN 26	Greenish brown	-	-	100	100
BN 27	Greenish brown	-	-	100	100
BN 28	Blackish grey	-	<1	99	99
BN 29	Earthy brown	-	77	21	98
BN 30	Greyish brown	-	80.6	19	99.6
BN 31	Yellowish brown	-	79.03	19	98.03
BN 32	Reddish brown	-	77.5	22.2	99.7
BN 33	Earthy brown	38.45	46	14.5	98.9
BN 34	Yellowish brown	-	90.1	8.9	99
BN 35	Greenish brown	-	48	51	99
BN 36	Earthy brown	-	76.1	23.1	99.1
BN 37	Earthy brown	-	90.1	9.3	99.4
BN 38	Earthy brown	-	89	10.26	99
BN 39	Earthy brown	-	64	35	99
BN 40	Earthy brown	-	39	60	99
BN 41	Earthy brown	-	82	17.6	99.6
BN 42	Greenish brown	-	73	26	99
BN 43	Earthy brown	-	63	36	99
BN 44	Greenish brown	-	77	22	99
BN 45	Greenish brown	-	65.8	33.45	99.25
BN 46	Earthy brown	-	95.5	4	99.5
BN 47	Earthy brown	-	85	13.8	98.8
BN 48	Greenish brown	-	79	20	99
BN 49	Greenish brown	-	69	29.1	98.1
BN 50	Earthy brown	-	88.9	9.9	98.9

sand-size fractions due to the porous and permeable behaviour of sandy soil and minerals present are less soluble in water leading to low salt content. Therefore, low TDS is caused by the presence of sand-size fraction in soil.

Distribution pattern of salinity: Two soil salinity increasing trends are observed. Both clusters occur on the East and Southwest of the Eastern Flank of Cape Monze anticline. The presence of high soil salinity towards the sea is due to the low relief topography of the area, the presence of clay size fraction and

Table 7: Specification for concrete exposed to varying soil sulfate content

Sulfate exposure	Water soluble sulfate (SO ₄) in soil (%)	Ordinary portland cement ASTM C 150	Maximum water to cement ratio	Maximum compressive strength (psi)
Negligible	0.00-0.10	OPC	0.45	-
Moderate	0.1-0.20	II	0.42	4500
Severe	0.2-2.00	V	0.40	5000
Very severe	>2.00	Type V+pozzolan	0.40	5000

seawater invasion as the river is replenished by salty seawater which tends to invade the soil causing high salinity in these sites. Whereas, soil salinity is lower on the West of LalBakhar Ridge (Benazirabad Town) due to the presence of a large amount of sand-dominated fraction.

Textural analysis of soil: The grain size distribution of collected soil samples has been summarized in Table 6. According to the AASHTO soil classification system, the soil is mainly comprised of fine sand (<10% passed from mesh 200) to sand-clay mixtures (maximum 79% retained and 60% passed from mesh 200) followed by calcareous gravelly sand to gritty clay where grits are comprised of limestone fragments.

Effect of cement type on concrete in Cl-SO₄ environment: Concrete is a porous material which is susceptible to the migration of highly deleterious species (SO₄ and Cl⁻). Extremely high concentrations of sulfate and chloride in a large number of collected samples can cause significant risks to concrete life and durability. According to ACI-350 B specification, a large number of sampling sites (n = 28) have severe sulfate exposures where ASTM C-150 type 5 OPC cement with only 5% C₃A content is recommended (Table 7). While, other sites fall in moderate sulfate concentration where ordinary Portland type II cement is specified with 0.42 w/c ratio and 8% C₃A content. Moreover, sites located in Benazir Abad Town have negligible sulfate concentration (0.04-0.08%) where, no special type of sulfate resisting cement is suggested. As per ACI 350B standard, soil which contains <0.1% sulfate concentration has a negligible effect on concrete life. On the other hand, ASTM type 5 OPC cement is highly corrosive for reinforcement steel as it fails to resist chloride attack at chloride concentration >0.1% in soil. Since low C₃A content in type V cement does not produce a significant amount of Ca(OH)₂ in cement paste to increase chloride binding capacity in the form of Friedel's salt 40. However, chloride concentration in a large number of samples (n = 39) is <0.1% where, type V OPC cement can be used to resist both Cl-SO₄ attacks. As compared to plain cement, blended cement performs better. Type 1 cement blended with 7% silica fume or 20% fly ash has the best corrosion resistance to type V²⁸.

CONCLUSION

The present study concluded that the soil is mainly alkaline and salinity distribution in the study area is uneven which is more elevated toward coastal parts. The presence of clay-dominated fraction and NaCl salt are causing high TDS towards the sea while low TDS is caused by a sand fraction. Hence, type II cement and type V cement as well as type I+7% silica fume or 20% fly ash are recommended in Hawks Bay Town and areas near Mubarak Village. Whereas, normal OPC cement is suggested for negligible sulfate exposure sites such as Benazir Abad Town. However, further studies are required to assess the increasing trend of soil salinity with >1 m depth for the construction of large buildings.

SIGNIFICANCE STATEMENT

This study discovers the distribution pattern of sulphate and chloride in coastal soil that will assist the planners and developers for construction by using the required cement type to inhibit corrosive elements (sulphate and chloride) for increasing the life of concrete structures in coastal cities. This study will help the researchers to classify the soil types chemically and recommend the corresponding cement type for concrete work.

REFERENCES

1. Roy, S. and S.K. Bhalla, 2017. Role of geotechnical properties of soil on civil engineering structures. *Resour. Environ.*, 7: 103-109.
2. Arulmathi, C. and G. Porkodi, 2020. Characteristics of coastal saline soil and their management: A review. *Int. J. Curr. Microbiol. Appl. Sci.*, 9: 1726-1734.
3. Metternicht, G.I. and J.A. Zinck, 2003. Remote sensing of soil salinity: Potentials and constraints. *Remote Sens. Environ.*, 85: 1-20.
4. Abuelgasim, A. and R. Ammad, 2019. Mapping soil salinity in arid and semi-arid regions using Landsat 8 OLI satellite data. *Remote Sens. Appl.: Soc. Environ.*, 13: 415-425.
5. Kumar, N., S.K. Singh and H.K. Pandey, 2018. Drainage morphometric analysis using open access earth observation datasets in a drought-affected part of Bundelkhand, India. *Appl. Geomatics*, 10: 173-189.
6. Youssef, A.M., B. Pradhan, A.A. Sabtan and H.M. El-Harbi, 2012. Coupling of remote sensing data aided with field investigations for geological hazards assessment in Jazan Area, Kingdom of Saudi Arabia. *Environ. Earth Sci.*, 65: 119-130.
7. Ehwailat, K.I.A., M.A.M. Ismail and A.M.A. Ezreig, 2021. Novel approach to the treatment of gypseous soil-induced ettringite using blends of non-calcium-based stabilizer, ground granulated blast-furnace slag and metakaolin. *Materials*, Vol. 14. 10.3390/ma14185198.
8. Firoozi, A.A., C.G. Olgun, A.A. Firoozi and M.S. Baghini, 2017. Fundamentals of soil stabilization. *Int. J. Geo-Eng.*, Vol. 8. 10.1186/s40703-017-0064-9.
9. Hozatloğlu, D.T. and I. Yılmaz, 2021. Shallow mixing and column performances of lime, fly ash and gypsum on the stabilization of swelling soils. *Eng. Geol.*, Vol. 280. 10.1016/j.enggeo.2020.105931.
10. Cai, G., S. Liu, G. Du, Z. Chen, X. Zheng and J. Li, 2021. Mechanical performances and microstructural characteristics of reactive MgO-carbonated silt subjected to freezing-thawing cycles. *J. Rock Mech. Geotech. Eng.*, 13: 875-884.
11. Ouhadi, V.R. and R.N. Yong, 2008. Ettringite formation and behaviour in clayey soils. *Appl. Clay Sci.*, 42: 258-265.
12. Nair, S. and D. Little, 2011. Mechanisms of distress associated with sulfate-induced heaving in lime-treated soils. *Transp. Res. Rec.: J. Transp. Res. Board*, 2212: 82-90.
13. Puppala, A.J., N. Talluri and B.C.S. Chittoori, 2014. Calcium-based stabiliser treatment of sulfate-bearing soils. *Proc. Inst. Civ. Eng. Ground Improv.*, 167: 162-172.
14. Aldaood, A., M. Bouasker and M. Al-Mukhtar, 2021. Mechanical behavior of gypseous soil treated with lime. *Geotech. Geol. Eng.*, 39: 719-733.
15. Abdi, M.R., A. Askarian and M.S.S. Gonbad, 2020. Effects of sodium and calcium sulphates on volume stability and strength of lime-stabilized kaolinite. *Bull. Eng. Geol. Environ.*, 79: 941-957.
16. Khadka, S.D., P.W. Jayawickrama, S. Senadheera and B. Segvic, 2020. Stabilization of highly expansive soils containing sulfate using metakaolin and fly ash based geopolymer modified with lime and gypsum. *Transp. Geotech.*, Vol. 23. 10.1016/j.trgeo.2020.100327.
17. Wang, L., J. Liu, X. Yu, X. Li, A.J. Puppala and Q. Wang, 2021. Experimental study on the correlation between the partial and total salt content in saline gravel using ion chromatography. *Transp. Geotech.*, Vol. 26. 10.1016/j.trgeo.2020.100424.
18. Caselles, L.D., J. Hot, C. Roosz and M. Cyr, 2020. Stabilization of soils containing sulfates by using alternative hydraulic binders. *Appl. Geochem.*, Vol. 113. 10.1016/j.apgeochem.2019.104494.
19. Chakkor, O., M.F. Altan and O. Canpolat, 2021. Metakaolin and red-mud based geopolymer: Resistance to sodium and magnesium sulfate attack. *Celal Bayar Univ. J. Sci.*, 17: 101-113.
20. Jiahui, P., Z. Jianxin and Q. Jindong, 2006. The mechanism of the formation and transformation of ettringite. *J. Wuhan Univ. Technol. Mater. Sci. Ed.* 21: 158-161.
21. Avwenagha, E. Oghenero, G.A. Enuvie and T.A. Celestine, 2014. Geotechnical properties of subsurface soils in Warri, Western Niger Delta, Nigeria. *J. Earth Sci. Geotech. Eng.*, 4: 89-102.
22. Youdeowei, P.O. and H.O. Nwankwoala, 2013. Suitability of soils as bearing media at a freshwater swamp terrain in the Niger Delta. *J. Geol. Min. Res.*, 5: 58-64.

23. Ngah, S.A. and H.O. Nwankwoala, 2013. Evaluation of sub-soil geotechnical properties for shallow foundation design in Onne, Rivers State, Nigeria. *Int. J. Eng. Sci.*, 2: 8-16.
24. Zhang, Y.Y., W. Wu and H. Liu, 2019. Factors affecting variations of soil pH in different horizons in hilly regions. *PLoS ONE*, Vol. 14. 10.1371/journal.pone.0218563.
25. Castrignanò, A., G. Buttafuoco, R. Comolli and A. Castrignanò, 2011. Using digital elevation model to improve soil pH prediction in an alpine doline. *Pedosphere*, 21: 259-270.
26. Al-Amoudi, O.S.B., 2002. Attack on plain and blended cements exposed to aggressive sulfate environments. *Cem. Concr. Compos.*, 24: 305-316.
27. Islam, M.S., 2019. Corrosion of steel in concrete due To chloride and sulphate attack. *North Am. Acad. Res.*, 2: 65-74.
28. Maslehuddin, M., M.M. Al-Zahrani, M. Ibrahim, M.H. Al-Mehthel and S.H. Al-Idi, 2007. Effect of chloride concentration in soil on reinforcement corrosion. *Constr. Build. Mater.*, 21: 1825-1832.
29. Karmakar, R., I. Das, D. Dutta and A. Rakshit, 2016. Potential effects of climate change on soil properties: A review. *Sci. Int.*, 4: 51-73.
30. Umasankareswari, T., V. Dharshana, K. Saravanadevi, R. Dorothy, T. Sasilatha, T.A. Nguyen and S. Rajendran 2022. Soil Moisture Nanosensors. In: *Nanosensors for Smart Agriculture: A volume in Micro and Nano Technologies*, Denizli, A., T.A. Nguyen, S. Rajendran, G. Yasin and A.K. Nadda (Eds.), Elsevier, Amsterdam, Netherlands, ISBN: 978-0-12-824554-5, pp: 185-216.
31. Ogunkunle, C.O., S. Oyedeji, H.K. Okoro and V. Adimula, 2021. Interaction of Nanoparticles with Soil. In: *Nanomaterials for Soil Remediation*, Amrane, A., D. Mohan, T.A. Nguyen, A.A. Assadi and G. Yasin, Elsevier, Amsterdam, Netherlands, ISBN: 978-0-12-822891-3, pp: 101-132.
32. Samtio, M.S., A.A.A.D. Hakro, R.A. Lashahri, A.S. Mastoi, R.H. Rajper and M.H. Agheem, 2021. Depositional environment of Nari formation from Lal Bagh section of Sehwan Area, Sindh Pakistan. *Sindh Univ. Res. J. SURJ*, 53: 67-76.
33. Hussain, S., M. Shaukat, M. Ashraf, C. Zhu, Q. Jin and J. Zhang, 2019. Salinity Stress in Arid and Semi-Arid Climates: Effects and Management in Field Crops. In: *Climate Change and Agriculture*, Hussain, S. (Ed.), IntechOpen, London, UK, ISBN: 9781789856675, Pages: 26.
34. Corwin, D.L. and E. Scudiero, 2019. Review of soil salinity assessment for agriculture across multiple scales using proximal and/or remote sensors. *Adv. Agron.*, 158: 1-130.
35. Xu, Z., S.W. Bassett, B. Hu and S.B. Dyer, 2016. Long distance seawater intrusion through a karst conduit network in the Woodville Karst Plain, Florida. *Sci. Rep.*, Vol. 6. 10.1038/srep32235.
36. Mukhopadhyay, S., R.E. Masto, R.C. Tripathi and N.K. Srivastava, 2019. Application of Soil Quality Indicators for the Phytoremediation of Mine Spoil Dumps. In: *Phytomanagement of Polluted Sites: Market Opportunities in Sustainable Phytoremediation*, Pandey, V.C. and K. Bauddh (Eds.), Elsevier, Amsterdam, Netherlands, ISBN: 978-0-12-813912-7, pp: 361-388.
37. Al-Busaidi, A.S. and P. Cookson, 2003. Salinity-pH relationships in calcareous soils. *J. Agric. Mar. Sci.*, 8: 41-46.
38. Wadu, M.C.W.M., V.K. Michaelis, S. Kroeker and O.O. Akinremi, 2013. Exchangeable calcium/magnesium ratio affects phosphorus behavior in calcareous soils. *Soil Sci. Soc. Am. J.*, 77: 2004-2013.